SPATIAL AND TEMPORAL SUMMATION IN THE DETECTION OF MOTION IN STOCHASTIC RANDOM DOT DISPLAYS

Cathryn J. Downing and J. Anthony Movshon
Dept. of Psychology and Center for Neural Science
New York University, New York, NY

Supplement to Investigative Ophthalmology and Visual Science, 1989,

vol. *30*, p. 72

Background

We describe a series of psychophysical observations on the detection and discrimination of motion signals presented in a field of dynamic visual noise. The target (see below) was designed so that judgements would have to be based on motion cues, in the hope that performance would depend on the function of a visual motion system like the one that has been identified in the primate visual cortex. Using this stimulus, Newsome and Paré (1988, *Journal of Neuroscience*) showed that lesions of visual area MT selectively elevated thresholds for detecting motion. Britten, Newsome and Movshon (1989, this meeting), also using the same target, have shown that behavioral thresholds for motion detection are similar to thresholds for reliable activation of neurons in MT. We sought to establish whether parametric variations in the density, area, duration, velocity and eccentricity of our motion target might provide further information about the processing of these signals.

Methods

Stimuli for these experiments were fields of dynamic random dots containing a coherent motion signal masked by noise. The dots are plotted in a continuous stream at a rate that determines the overall dot density of the display. Within the stream, there are two kinds of dot: *random* dots, plotted at locations uncorrelated with any prior dot, and *correlated* dots, plotted at a specific spatial and temporal offset (Δx and Δt) from a prior ''remembered'' dot. The probability that a dot has a successor controls the strength of the motion signal at that velocity. When this probability is zero, we expect no motion signal at the target velocity, because no dots will be paired with another dot at the specified Δx and Δt. This is the case represented in the leftmost panel of Figure 1. When the probability is unity, we expect a strong motion signal, because all dots (after their initial appearance at random locations) are constrained to give rise to a succession of dots, each at the specified offset from its predecessor. This is represented in the rightmost panel. The strength of the motion signal will vary between these two extremes for intermediate probability values. A sample display for a succession probability of 0.5 is depicted in the central panel.

We suppose that the detection of motion in this pattern is related in some way to the number of dot-pairs that carry a particular motion signal. We can calculate the *expected number of signal pairs* that will appear in any stimulus display, and use it to indicate the strength of the motion signal at the target velocity. This is not simply proportional to the succession probability, but depends also on the relation between the size of the spatial and temporal offsets and the size and duration of the display itself.

The task required the subject to indicate which of four stimulus patches — typically centered 5 deg from the center of gaze along the oblique axes of the visual field — contained a coherent motion signal (see Figure 2). In three of the patches, the succession probability was zero. In the fourth, it was adjusted according to a staircase procedure set to converge at a threshold performance of 50% correct. The location of the signal patch was chosen at random. The direction of the motion in the signal patch was also chosen at random, either from a set of eight (major axes and obliques) or four directions (major axes only). Preliminary studies showed that neither the direction of motion nor the quadrant of the visual field in which the stimulus was placed had an appreciable effect on motion thresholds. We varied dot density between 12 and 167 dots/deg^2/sec. For all data presented here, the Δt between signal dots was 45 msec. The tested values of Δx ranged from 0.04 to 1.2 deg, with a corresponding speed range from 0.9 to 26.7 deg/sec. The stimulus areas that we examined ranged from 0.25 to 52 deg^2, and the stimulus durations from 0.125 to 4.0 sec. In a subsequent series, we also varied the eccentricity of the stimuli from 0.7 to 8.5 deg.

Figure 1. The motion stimulus used in these experiments.

Figure 2. The arrangement of viewing areas in the display.

Figure 3. Three graphs showing the results of a set of measurements in which the area and dot density of the display were varied. The left-hand panel shows the thresholds plotted in units of signal pairs S, defined as the expected number of signal dot-pairs in the stimulus. Each symbol in the figure represents thresholds for stimuli at one of the five dot densities that we tested. The dot density associated with each symbol, in dots/deg^2/sec, is indicated to the left of each curve in the first panel. The middle panel shows the same thresholds plotted in terms of the *density* of signal dot-pairs $S/\text{deg}^2/\text{sec}$. The right-most panel shows the same thresholds a third time, plotted in terms of an approximate *signal-to-noise ratio*, given as the ratio of signal dot-pair density S to background dot density D.

It is evident that expressing thresholds in units of S/D causes the data to overlie one another very closely, suggesting that performance is limited by signal-to-noise considerations. We express threshold in units of S/D for the remaining figures in this presentation.

The data reveal that performance improves gradually with the area of the stimulus, up to an area of roughly 25 deg^2.

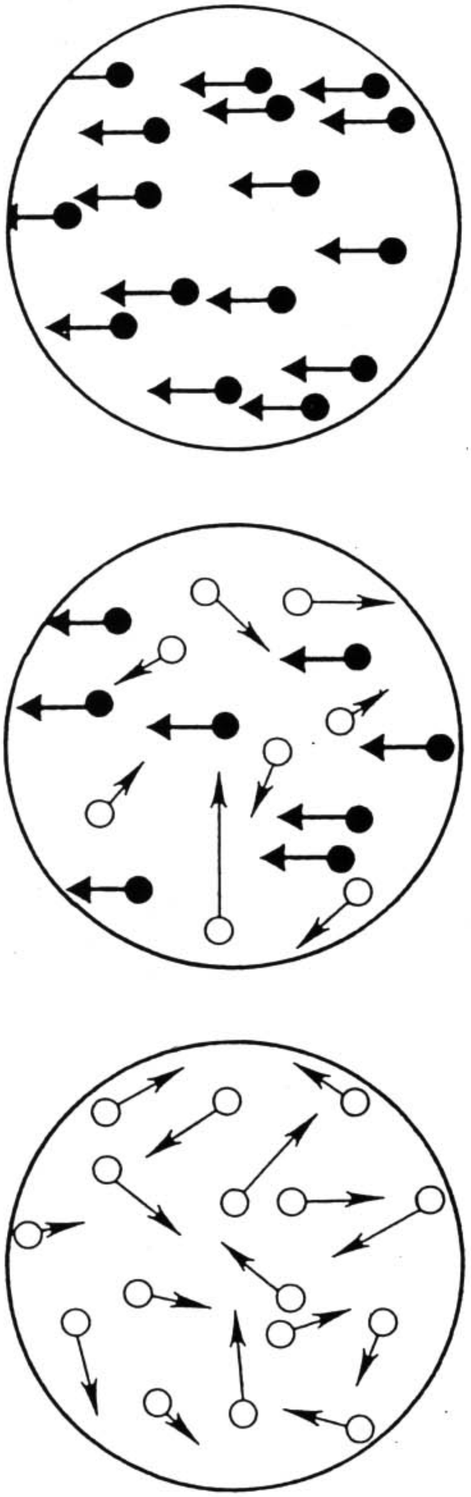

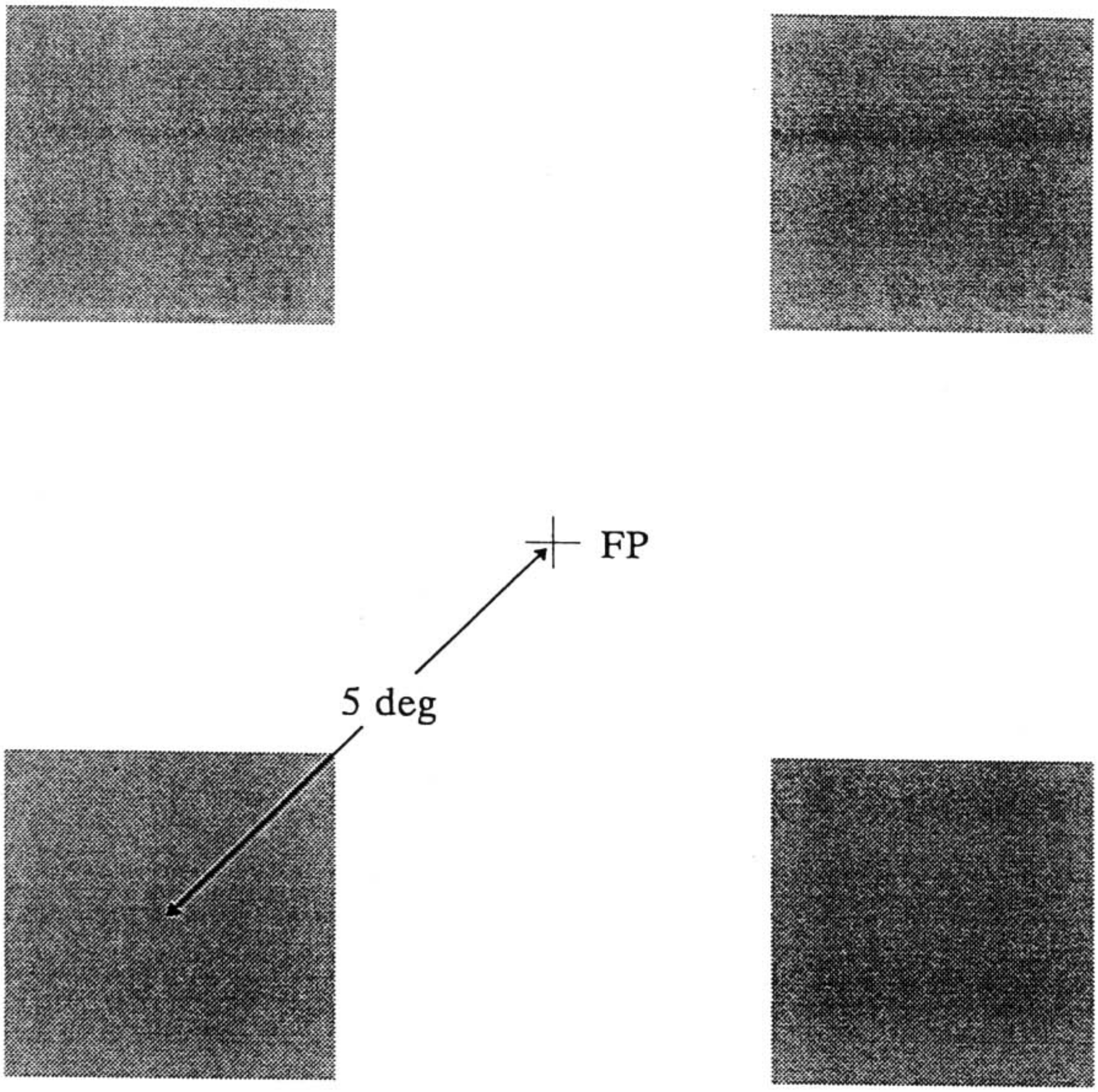
FP
5 deg

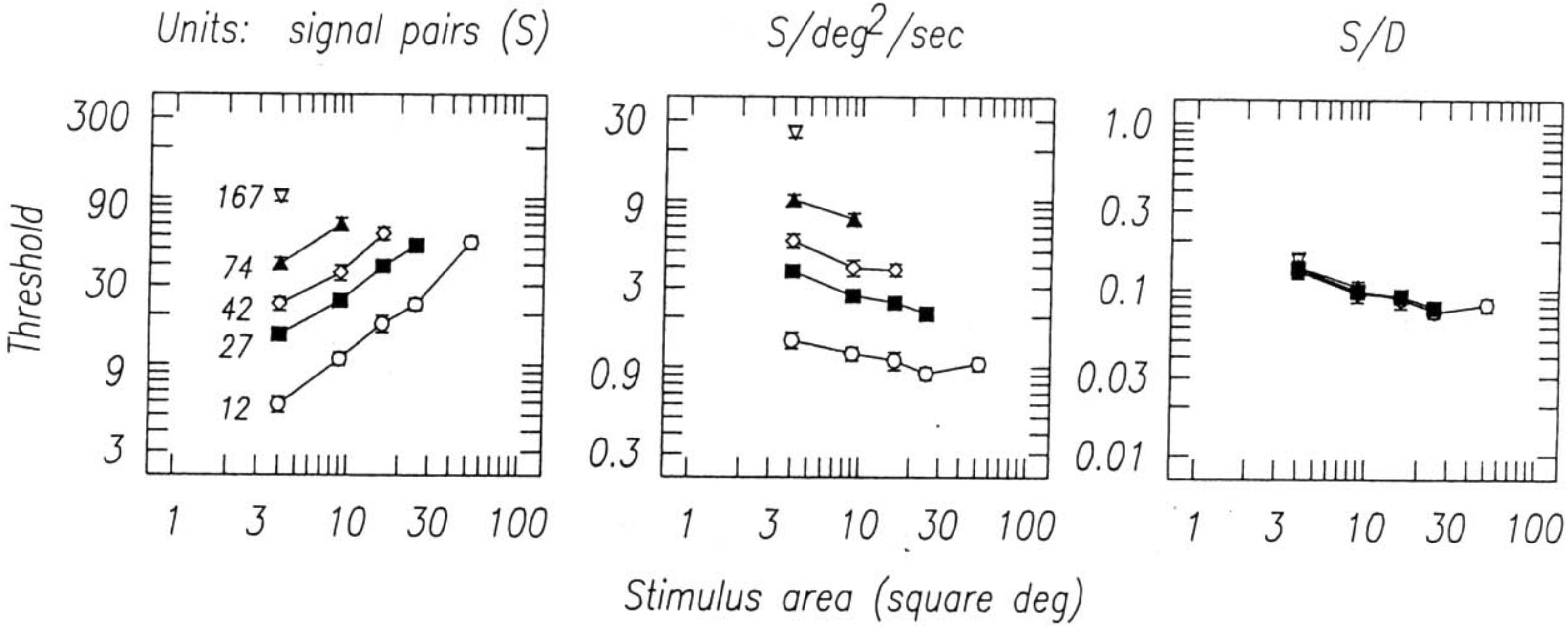
Units: signal pairs (S)
S/deg^2/sec
S/D
Threshold
300
90
30
9
3
167
74
42
27
12
30
9
3
0.9
0.3
1.0
0.3
0.1
0.03
0.01
1
3
10
30
100
Stimulus area (square deg)

Figure 4. Evaluation of the effects of stimulus area and duration. In this series of tests, dot density was held constant at 12 dots/deg^2/sec, while stimulus area ranged from 4 to 52 deg^2 and stimulus duration ranged from 0.125 to 2 sec. The left-hand panel shows that thresholds fall gradually with area up to roughly 25 deg^2 for all stimulus durations; the relation is similar to that shown in Figure 3. The right-hand panel shows that thresholds fall smoothly and somewhat more rapidly with duration (following approximately a square-root law for durations up to 0.5 - 1 sec).

All the curves in each panel seem to be vertically shifted replicas, suggesting that there is no important interaction between the effects of area and duration. We conclude that — neglecting the effects of spatial and temporal probability summation — the characteristic area of spatial summation is about 25 deg^2 at our standard eccentricity of 5 deg. The characteristic duration of temporal summation is between 0.5 and 1 sec.

Figure 5. Measurements showing the velocity dependence of motion thresholds. We varied the spatial offset of the dot-pairs (Δx), while keeping Δt constant at 45 msec, to vary velocity. In each panel the velocity tuning for a large, long-duration stimulus (25 deg^2, 1 sec) is shown (displaced vertically downward) for reference.

The two panels show that velocity tuning depends little on either the area or the duration of the test field. The left-hand panel shows the results obtained for 7 stimulus areas ranging from 0.25 to 16 deg^2. The right-hand panel shows results for 5 durations ranging from 125 msec to 4 sec.

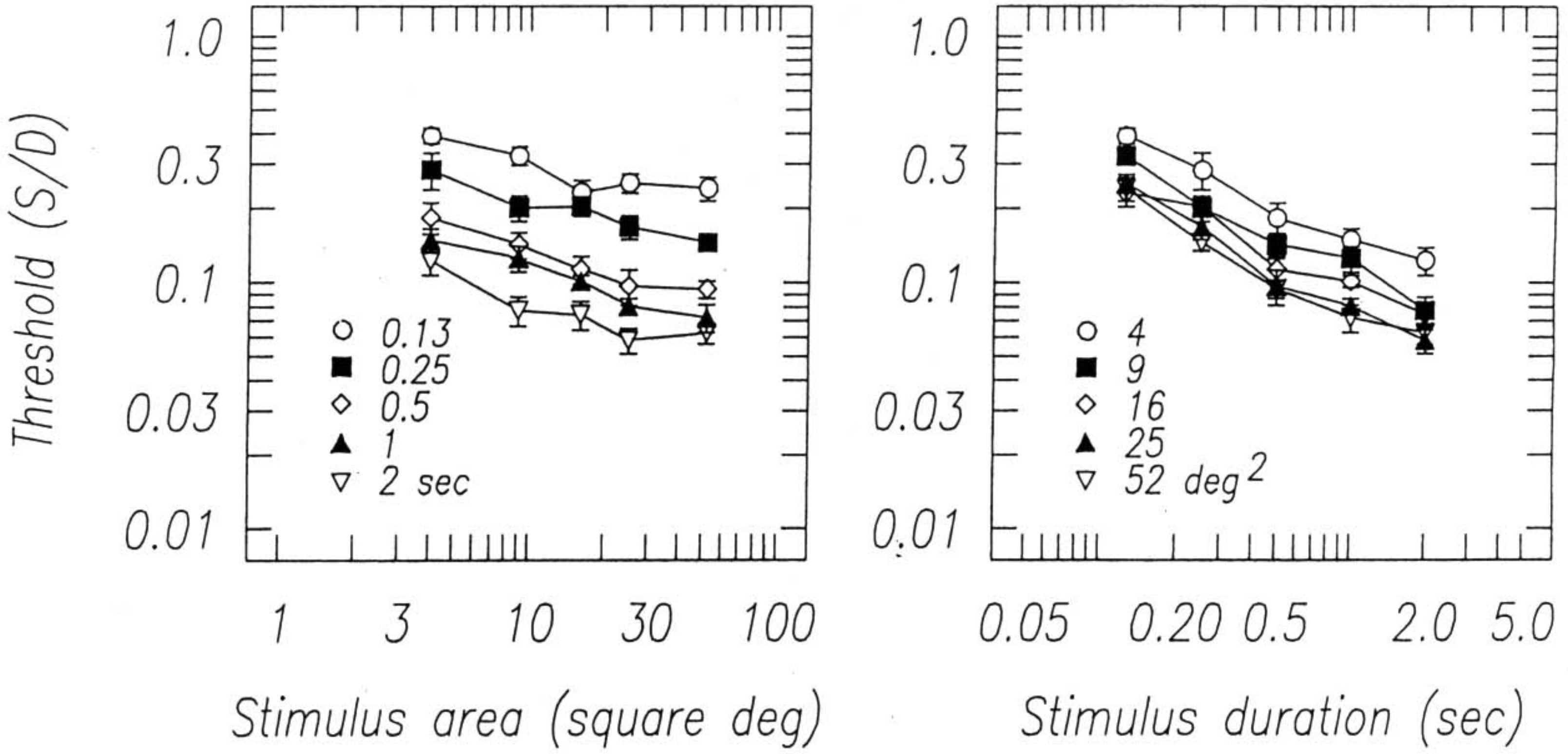
Threshold (S/D)
1.0
0.3
0.1
0.03
0.01
○ 0.13
■ 0.25
◇ 0.5
▲ 1
▽ 2 sec
1
3
10
30
100
Stimulus area (square deg)
1.0
0.3
0.1
0.03
0.01
○ 4
■ 9
◇ 16
▲ 25
▽ 52 deg 2
0.05
0.20
0.5
2.0
5.0
Stimulus duration (sec)

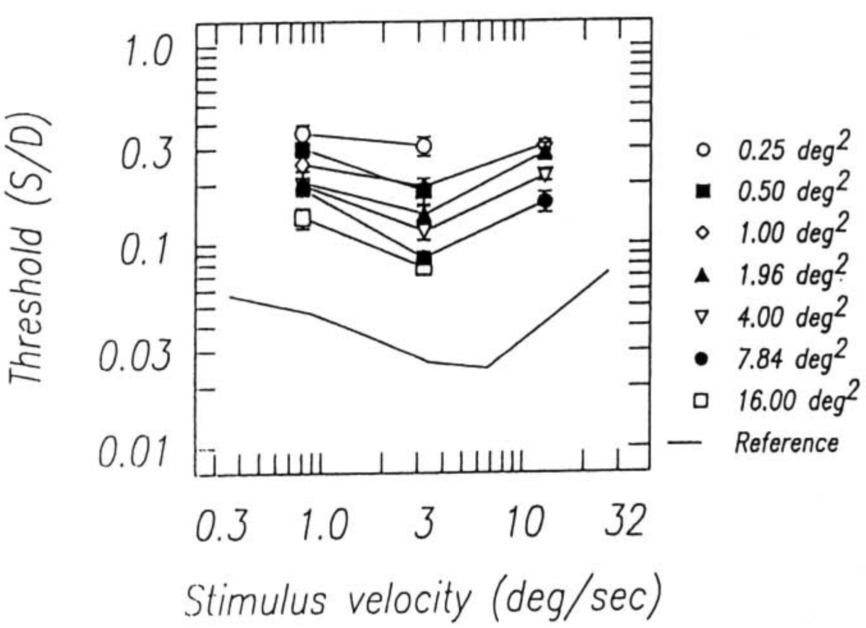
Threshold (S/D)
1.0
0.3
0.1
0.03
0.01
0.3
1.0
3
10
32
Stimulus velocity (deg/sec)
○ 0.25 deg^2
■ 0.50 deg^2
◇ 1.00 deg^2
▲ 1.96 deg^2
▽ 4.00 deg^2
● 7.84 deg^2
□ 16.00 deg^2
— Reference

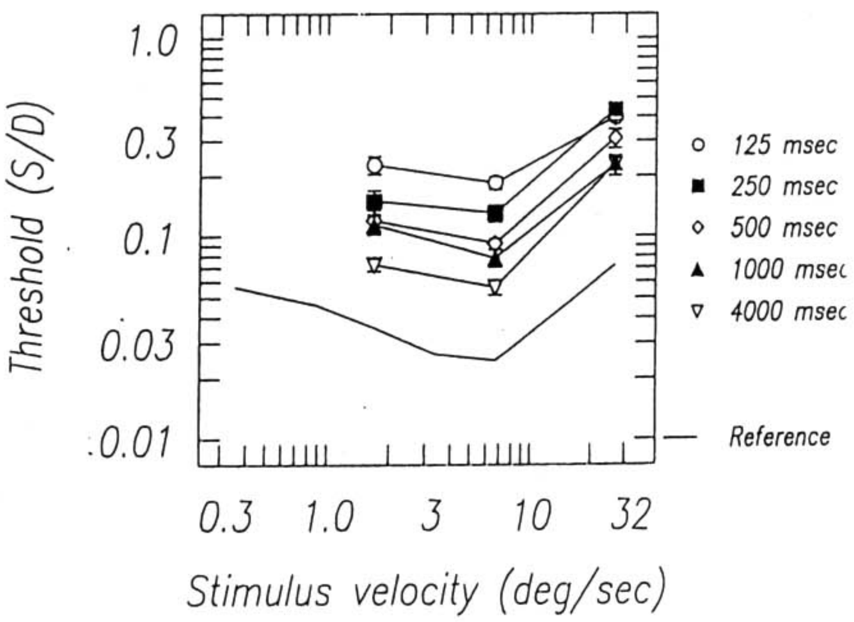
Threshold (S/D)
1.0
0.3
0.1
0.03
0.01
0.3
1.0
3
10
32
Stimulus velocity (deg/sec)
○ 125 msec
■ 250 msec
◇ 500 msec
▲ 1000 msec
▽ 4000 msec
— Reference

Figure 6. We were interested in knowing whether performance under all our conditions reflected the activity of mechanisms capable of discriminating *motion.* We used a 4×4 forced-choice procedure to measure detection and discrimination thresholds on the same sets of trials — the subject had to report both the panel containing stimulus motion, and the direction of the motion. A sample series showing the two types of thresholds for a series of stimuli varying in area (left panel; velocity 3.3 deg/sec; duration 1 sec; density 48 dots/deg^2/sec) reveals that they were indistinguishable.

The second panel shows the distribution of the ratio of detection to discrimination thresholds obtained for all the sessions we ran employing this paradigm (the parameters studied included dot density, area, velocity, and eccentricity). There seems to be no systematic deviation from equality.

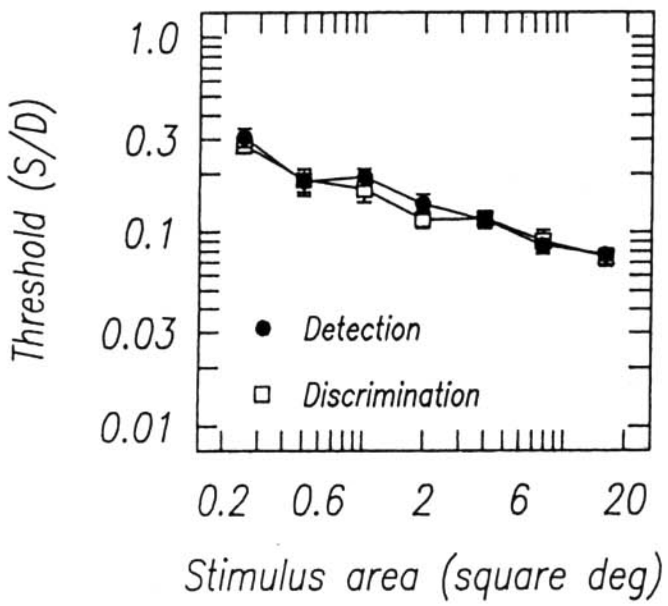

Threshold (S/D)
1.0
0.3
0.1
0.03
0.01
● Detection
□ Discrimination
0.2
0.6
2
6
20
Stimulus area (square deg)

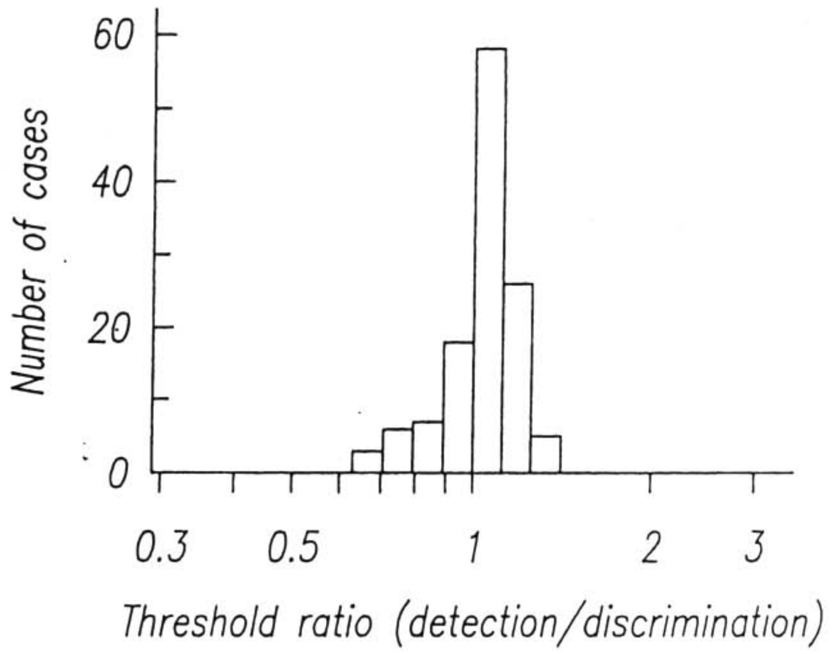

Number of cases
60
40
20
0
0.3
0.5
1
2
3
Threshold ratio (detection/discrimination)

Figure 7. In a final series of observations, we varied the eccentricity of 1 deg^2 stimulus patches along the oblique axes of the visual field. We expected that thresholds would be lower for stimuli positioned in the central visual field than for stimuli positioned more peripherally. This follows from the observation that within a topographically organized visual area, the region of cortex that is activated by stimulation of a point in the visual field, the *point image size*, varies with eccentricity. In areas such as V1, which contain cells with small receptive fields, point image size falls very rapidly with eccentricity. In areas such as MT, which contain cells with very much larger receptive fields, the point image size remains large and roughly uniform, even for stimuli some distance from fixation. The exact eccentricity at which point image size begins to fall depends strongly on the size and scatter of receptive fields centered at fixation.

The left-hand panel shows the width of the part of MT that would be activated for points at different eccentricities (our calculations are based on measurements by Albright and Desimone, 1987, *Experimental Brain Research*). On the assumption that thresholds would be lower when more cells in higher-order visual areas are available to process the motion signal, we would expect the curve showing thresholds over eccentricity to be qualitatively similar to this point image size function, but inverted. The thresholds shown in the right-hand panel do show such a trend, although they first begin to rise at larger eccentricities than we might expect from measurements of macaque MT. They clearly do not rise sharply with eccentricity, as would be expected if performance depended on the number of *V1* neurons whose receptive fields include the stimulus.

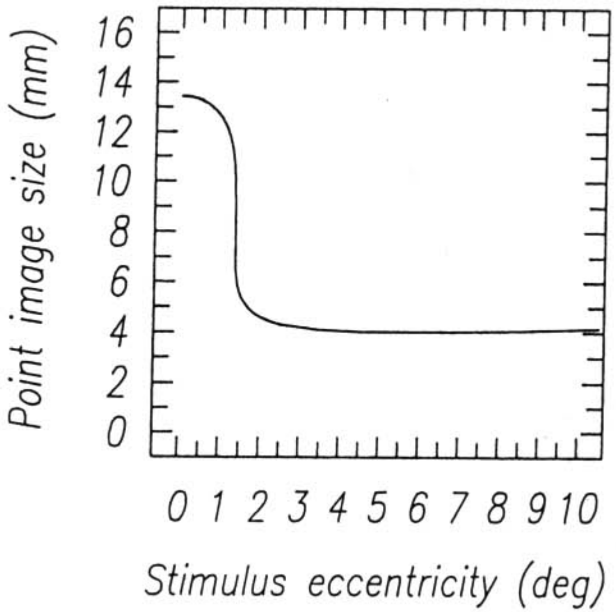
Point image size (mm)
16
14
12
10
8
6
4
2
0
0 1 2 3 4 5 6 7 8 9 10
Stimulus eccentricity (deg)

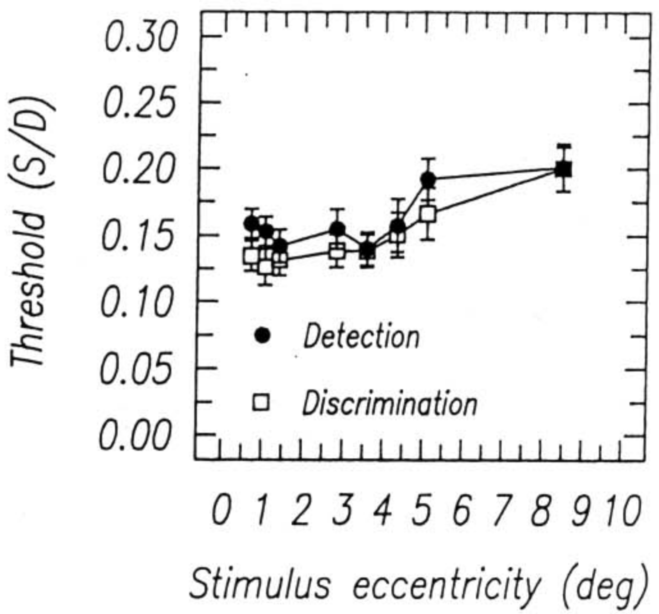
Threshold (S/D)
0.30
0.25
0.20
0.15
0.10
0.05
0.00
● Detection
□ Discrimination
0 1 2 3 4 5 6 7 8 9 10
Stimulus eccentricity (deg)

Conclusions

Our experiments sought to examine the dependence of thresholds for detecting and discriminating motion in this target upon the density, area, duration, velocity and eccentricity of the stimulus. Our results suggest that performance in our tasks depends on signals that are integrated over substantial areas and durations, and whose dependence on eccentricity bears a qualitative similarity to measures of spatial scale in primate MT. We conclude that this form of motion analysis depends on higher-order visual centers specialized for the analysis of visual motion, and that targets of this kind can be used to probe the functions of the primate ''motion pathway''.